Structural Assessment of an Internal Fixation System for a Forearm Long Bone Mid-shaft Fracture

MyKal Woody

Savannah State University, Department of Engineering Technology
3219 College St. Savannah, GA 31404

Abstract

A novel low cost manufacturing method for bone replicas is developed in order to provide cross sectional geometry for 3-D modeling. A Finite Element Analysis (FEA), based on this geometry, is used to predict stress distributions in the radius with and without an internal fixation device attached. The changes in stress distribution under tensile and torsional loads are quantified and agree well with predictions in current literature where more expensive modeling techniques are used. Normal stresses near the radial cortex are seen to be higher with the fixation device, however stress gradients are substantially steeper resulting in lower tensile stresses with decreasing as radial distance. Shear stress minimum values increase with the presence of the plates and do not reverse direction as is the case with the un-plated radius. Stress shielding effects due to the plates and stress concentrations due to the holes are observed to significantly affect stress magnitude and distribution in the radius bone with a fixation device. The results from this research support the conclusion that fixation devices leave bones more susceptible to future injury.

Keywords: Internal Fixation, Radius, Finite Element, fracture, repair

1. Introduction

Accidents and their resulting injuries are everyday occurrences. For persons with physically demanding careers (athletes, construction workers etc.), the occurrence and severity of these injuries are higher than normal. The radius is one of two long bones (the other being the ulna) in the forearm which transmit and distribute loads from the wrist to the elbow. A typical mid-shaft fracture is repaired using Dynamic Compression Plates (DCP) as shown in Figure 1. The DCP system provides compressive stresses as well as stability at the fracture interface. These phenomena improve bone union and decrease external callus formation during healing. Once the fracture has fully healed, the ability of the forearm to fully function may be reduced due to the presence of the plate and/or screws, improper union, or callus formation. If the patient requires full use of the forearm for his or her career, inadequate forearm function after surgery and bone healing may potentially trigger a lawsuit against the operating surgeon or group. This may occur even if the patient was advised of potential surgical complications prior to surgery. More importantly, substantial loss of forearm use may significantly reduce the quality of life and health of the patient. It is therefore essential to understand the internal changes in the bone that may occur if plates are retained after the bone has healed.

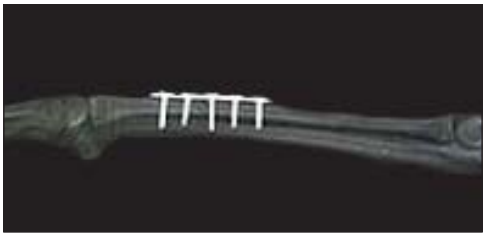

Figure 1. Dynamic compression plate applied to an ulna mid-shaft fracture (Reprinted with permission from Wheeless Textbook of Orthopedic Surgery)

1.1 Other Literature

When modeling bones for testing, several variables need to be considered. Martin[1] presented a mathematical model that could be histologically measured and related to the mechanical properties which determine bone function. The model aided in studying phenomena such as Wolff's Law[2], regional acceleratory phenomena, and fluorochrome label escape errors. Properties of the trabecular bones were treated as variables in this work. By comparing prism and cube-based cell types, Kowalczyk[3] parameterized elastic properties for the trabecular bone as FE models. Other literatures published on the subject of fixation devices have analyzed their performance. Gardener et al.[4] characterized the stiffness of the Orthofix DAF (Dynamic Axial Fixator), an external fixation device, using a mathematical stiffness matrix. The analysis provided the means of analyzing inter-fragmentary motions that arise from physiological loading, regardless of complexity. Conjunctly, Claes et al[5] provided a complete description of fixation stiffness needed to predict inter-fragmentary movement and potential effectiveness of device configurations. Results from the above investigations may provide insight into the FE results of this work on long bone performance with fixation devices.

1.2 Overview

In this work, Finite Element (FE) models of the radius and ulna bones with and without fixation devices are developed. The radius and ulna are restrained at the proximal ends and loaded at the distal ends in tensile and torsional modes. The load types used in the FE model simulate typical forearm usage during daily activity.

An inexpensive manufacturing method is also developed for suitable radius and ulna replicas. The replicas, made from lightweight plaster, are derived from geometrically correct plastic models. The method employs a manual counterpart to the cat scanning technique in order to obtain 2-D images to be extruded into a 3-D model.

2. Procedure

2.1 Manufacturing Method

This research introduces a cost-efficient way to replicate and transfer the radius and ulna geometry into CAD software. The process utilized Woodland Scenics lightweight Hydrocal, modeling clay, and talcum powder to create the bone replicas. In order to prevent adherence of clay to bone, the bone was lightly powdered with talcum powder. Modeling clay was then wrapped around the bone leaving the most irregularly shaped end of the bone exposed. With a scalpel the modeling clay was carefully cut in two halves. Once the bone was removed from the clay, both halves were evenly pressed together. The process is repeated for the irregularly shaped end in order to obtain a full sized replica. Figure 2 shows an exploded view of the long bone enclosed in two clay molds.

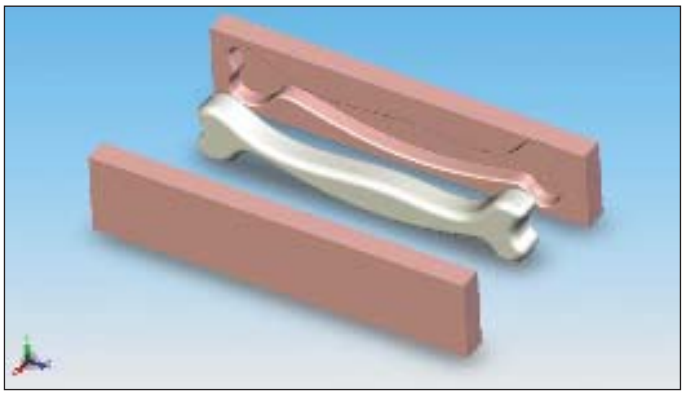

Figure 2. Clay molds and plastic bone used to create replicas

2.2 Replication of the Bone Model

The Hydrocal mixture was created by adding water to the powder in a 3/5^{ths} mixture of water to powder. This resulted in a softer material upon curing such that slicing could be accomplished successfully. Once the paste was poured into the mold, air bubbles were removed by lightly shaking it. The model was then allowed to dry overnight in an upright position. The replicas were cut into one-inch sections and marked with a T on the tops for orientation purposes. All cross sectional slices were scanned in order to provide 2-D images to be imported into a 3-D modeling software package (SolidWorks). Some of these cross sections are shown in Figure 3. The conversion factor for the model was created by dividing the actual measurement of the marker by the measurement of the marker in SolidWorks. A measurement of the marker in SolidWorks was obtained by measuring it with a line segment.

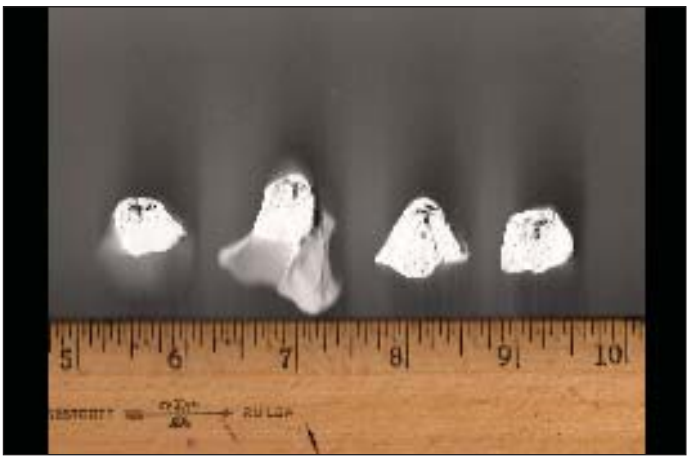

Figure 3. Scanned cross sectional slices for the radius model

Once all images were imported into SolidWorks and properly scaled, splines were sketched along their perimeters in their respective planes. Each plane was separated by one inch. To make the cortical and trabecular parts of the bones, the basic radius was copied three times. All of them were converted into either the cortical bone, left-end of the trabecular bone, or right-end of the trabecular bone. The original sketches were copied and resized to one fourth of their original size at the ends of the cortical bone and the area in the middle was reduced by half of the original size. Each cross-sectional sketch was extruded by 0.2mm to create profiles for lofting.

Screws were made in a similar fashion. The head of the screw was created from sketches of concentric circles that were lofted together. The top circle has a diameter of 5.0mm, the middle 6.0mm, and the bottom 3.5mm. By extruding the bottom circle to another circle 18.0mm below it, the shaft was created. Threads for the screw are created using the cosmic thread command and the 3.5mm circle at the end of the shaft.

The plates for the fixation device were created by extruding a rectangular sketch 3.3mm. Six circles were sketched on the plane on the top face of the plate. These circles were in two groups, starting 10.4mm from the (proximal/distal) ends of the plate and spaced an additional 10.4mm apart from each other. Each circle was cut-extruded through the plate and lined with the threads using the cosmic thread command.

3. FE Model

3.1 Numerical Properties

Separate models of the radius with and without an attached DCP fixation system were developed. The plate and screws were modeled as being perfectly bonded to the bone as well as each other, therefore no relative movement between bone and plate was allowed. The cortical bone was modeled as isotropic, while the trabecular bone was modeled as an orthotropic material. The Young's modulus and Poisson's ratio values used for the cortical bone were respectively, 11.4 (MPa) and 0.29.[6] Trabecular bone material properties in their respective x, y and z-directions were: Elastic Modulus, 239 MPa, 309 MPa, 823 MPa; Poisson's ratio 0.169, 0.063, 0.423; and Shear Modules, 73 MPa, 134 MPa, 112 MPa.[7]

A semi-course mesh with solid tetrahedronal elements was used for both models. The plated model consisted of 37,222 elements while the un-plated model consisted of 25,000 elements. The elements used were Jacobian in order to compensate for the nodes that contact on irregular edges. Bones were restrained at their proximal end under a cantilever condition. A 10N force was applied at the distal end for all bones. The force was applied axially in order to simulate a tensile load. A 1 N.m couple was also separately applied at the distal end in order to simulate a torsional load. The 3-D plated radius model used in the FE analysis, as well as a plated ulna model also developed, is shown below in Figure 4.

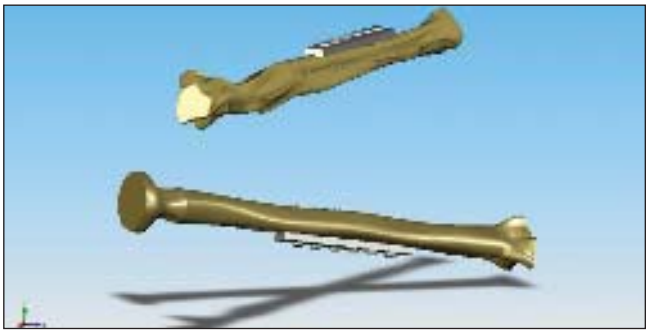

Figure 4. FE model of plated radius and ulna bones

3.2 FE validation

The mesh size was varied between course and fine to check for convergence. It was observed that stress results did not very substantially with mesh sizes finer than the semi-course mesh used. Additionally, an FEA of a hollow cylinder was developed using the same type of element and approximately the same number of elements. The tube was modeled using cortical bone properties only. Stress results for the cylindrical tube under tensile and torsional load agreed well with theoretical calculations.

4. Results & Discussion

All results obtained from the FE analysis are graphed as stress vs. distance, measured from the surface inward towards the center of the bone. These graphs capture the local changes in the stress along planes transverse to the bone's longitudinal axis. They also allow for observation of general trends in the stress distribution which may have arisen due to the presence of the plates.

4.1 Tensile Load Results

For descriptive purposes, we will define the mot proximal screw as the "first" screw position. Figure 5 shows a plot of the normal stress distribution along three transverse planes (series 1-3) for the plated bone. The 1st plane (series 1) is located on the proximal side of the first screw position; the second plane (series 2) is between the first and second screw, and so on. Figure 6 shows a similar plot for the un-plated radius. Based on Figures 5 and 6, the presence of the fixation device results in initially higher stresses near the cortex, however there is a substantial drop in these magnitudes at locations further inward. Normal stress values drop by as much as 80% at approximately 12mm from the cortex of the plated bone (Figure 5). Conversely, there is little or no normal stress reduction in the plated bone at

corresponding locations (Figure 6). It can also be observed that the difference in the normal stress values at equidistant points (from the longitudinal axis) on different planes is substantially smaller for the plated bone. For example, near the surface of the un-plated bone (x = 0), the normal stress values differ by as much as 26% (series 2 vs. series 3), while the plated values maximum difference is approximately 7% at x = 0.

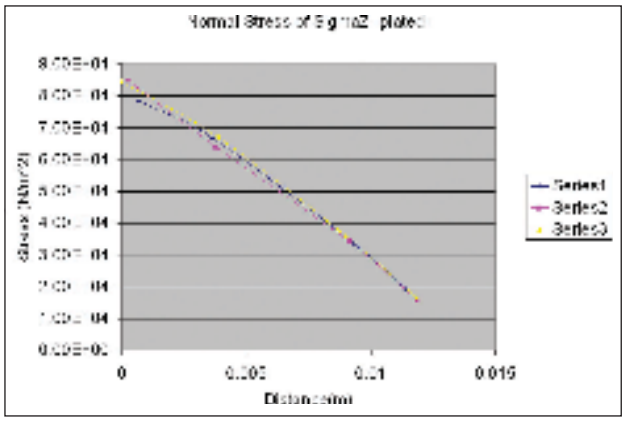

Figure 5. Normal stress distribution: plated radius under tensile load

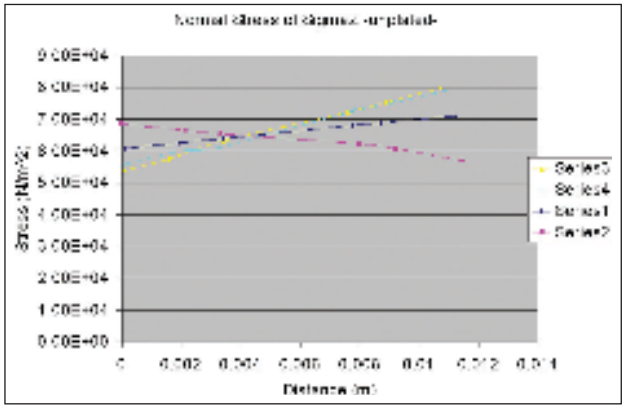

Figure 6. Normal stress distribution: un-plated radius under tensile load

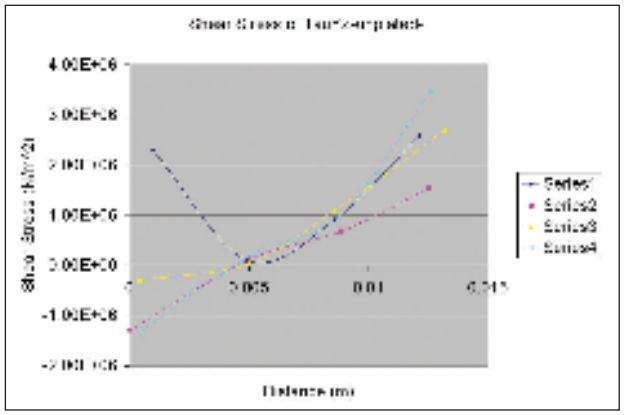

Figure 7. Shear stress distribution: un-plated radius under torsional load

4.2 Torsional Load Results

Figures 7 and 8 show the shear stress distribution along the same planes (defined in section 4.1) for the un-plated and plated bones respectively. The graphs show that the absolute values of the shear stresses in the un-plated and plated bones decrease to minimum values around 5 mm from the cortex and then increase further inward. The shear stress values and trends do not appear to change substantially with the presence of the fixation device. However, the plates do increase the minimum shear value (absolute) attained along the planes furthest from and closest to the applied load. Additionally, once this minimum value is attained, the shear direction is observed to reverse along three planes in the un-plated bone (series 2-4, Figure 7). This reversal only occurs on one plane in the plated bone (series 2, Figure 8). For the plated bone, the shear stresses along the planes closest to and furthest from the applied load do not reverse direction with increasing distance inward.

5. Conclusion

The decreased normal stress with the presence of the plates supports the concept of stress shielding advocated be many authors.[8, 9] Stress shielding implies that the plate takes some of the load away from the bone. The consequences of stress shielding however may be detrimental to bone strength as bone will remodel and adapt to the level of stress that is placed on it (Wolff's law). The steep stress gradients created due to the presence of the plates may also result in high density or strength gradients. This fact should be of concern to patients and surgeons as this increases the likelihood of micro-cracks during strenuous repetitive activity. Since the model did not account for slippage between plate and bone, it is a conservative one. Relative slippage would introduce added shear stress near the cortex and contact stresses, which may affect bone vascularity.[10] These FE results indicate that plate retention after the fracture has healed may result in a bone that is more susceptible to micro-cracks and reduced density in the vicinity of the plates.

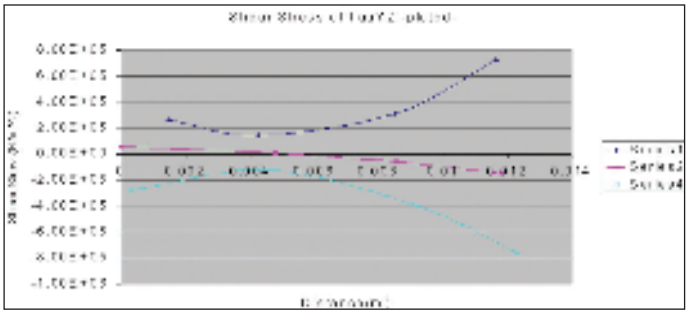

Figure 8. Shear stress distribution: plated radius under torsional load

Acknowledgments

This research was performed at Armstrong Atlantic State University (AASU) as a component of the Minority Access to Graduate Education and Careers in Science, Technology, Engineering, and Mathematics (MAGEC-STEM) program at Savannah State University (NSF grant #0310328). I would like to thank my research mentor, Dr. Cameron Coates, of AASU, for his supervision of this project and am also grateful to the Georgia Space Grant Consortium for providing partial funding for this work.

References

[1] Martin, R.B. The Usefulness of Mathematical Models for Bone Remodeling. *YearBook of Physical Anthropology* **1985**, 28(S6), 227-236.

[2] Pearson O. M.; Lieberman D.E. The Aging of "Wolff"s Law": Ontogeny and Responses to Mechanical Loading in Cortical Bone. *YearBook of Physical Anthropology* **2004**, 47, 63-69.

[3] Kowalczyk, P. Elastic properties of Cancellous Bone Derived from Finite Element models of parameterized microstructure cells. *Journal of Biomechanics*. **2003**, 36(7), 961-972

[4] Gardner, N. T.; Weemaes, M. A mathematical stiffness matrix for characterising mechanical performance of the Orthofix DAF. *Medical Engineering & Physics* **1999**, 21(2), 65-71

[5] Claes, L.; Duda, N. G.; Wilk H.; W. Helmut, K. A Method to Determine the 3-D Stiffness of Fracture Fixation Devices and its Application to predict Inter-fragmentary Movement. *Journal of Biomechanics*. **1997**, 3:31, 247-252.

[6] Tencer .F. and Johnson K.D. Biomechanics of Orthopedic Trauma; Martin Dunitz Ltd: London; 1994; pp. 31.

[7] Keveany T.M.; Morgan E.F.; Niebur .L.; Yeh O.C. Biomechanics of Trabecular Bone. *Annual Review in Biomedical Engr*.**2001**, 307-33.

[8] Ganesh, V.K.; Ramakrishna K.; Ghista, D.N. Biomechanics of bone-fracture fixation by Stiffness-graded Plates in Comparison with Stainless-Steel Plates. *Biomedical Eng Online* 2005, 4, 46.

[9] Cheal E.J.; Hayes W.C.; White III A.A.; Perren S.M. Stress Analysis of Compression Plate Fixation and its effect on long term Remodeling. *Journal of Biomechanics* **1985**, 18, 141-150.

[10] Perren, S.M.; Cordey J.; Rahn B.A.; Gautier E.; Schneider E. Early Temporary Porosis of Bone Induced by Internal Fixation: A reaction to neurosis, not to stress protection. *Clinical Orthopedics and Related Research* **1988**, 232, 139-151.

About the Author

Mykal is a sophomore at Savannah State University majoring in mechanical engineering with a minor in engineering management. Mykal was born and raised in Atlanta, GA.

Mykal is a Minority Access to Graduate Education and Careers in Science Technology Engineering and Math (MAGEC-STEM) scholar. Mykal recently received 1st place for my oral presentation in the Peach State Louis Stokes Alliance for Minority Participation (PSLSAMP) Fall Forum and Research Conference.

Mykal intends to work as a mechanical engineer for a company that allows me to grow technically and provides increasing leadership responsibilities. Mykal plans to complete a Master's degree in Engineering while working and eventually create and run an engineering business.